Polymer Chemistry

ROYAL SOCIETY OF CHEMISTRY

PAPER

View Article Online
View Journal | View Issue

Cite this: *Polym. Chem.*, 2021, **12**, 3939

Mesoporous polyetherimide thin films *via* hydrolysis of polylactide-*b*-polyetherimide-*b*-polylactide†

Dong Guo, [a] Jocelyn Riet,[b] Assad Khan, [a] Yichen Guo,[a] Zhen Xu,[a] Tianyu Liu [a] and Guoliang Liu *[a,c,d]

Received 6th May 2021,
Accepted 20th May 2021

DOI: 10.1039/d1py00601k

rsc.li/polymers

Mesoporous polyetherimides are important high-performance polymers. Conventional strategies to prepare porous polyetherimides, and polyimide in general, are based on covalent organic framework or thermolysis of sacrificial polymers. The former produces micropores due to intrinsically crosslinked microstructures, and the latter results in macropores because of a blowing effect by the sacrificial polymers. The preparation of mesopores remains a challenge. Here we have prepared mesoporous polyetherimide films by hydrolyzing polylactide-*b*-polyetherimide-*b*-polylactide (AIA). Controlled by molecular weight and volume fraction of polylactide in AIA, the porous films exhibit an average pore width of 24 nm. The mesoporous polyetherimide films exhibit a storage modulus of ~1 GPa at ambient temperatures. This work advances the chemistry of high-performance polymers and provides an alternative strategy to prepare mesoporous polymers, enabling potential use as high-performance membranes for separation, purification, and electrochemistry.

Introduction

Porous polyimides (PIs) are high-performance engineering materials with broad applications in gas separation,[1–6] CO_2 capture,[7–14] water purification,[15,16] oil retention,[17–19] catalysis,[20] microelectronics,[21–26] and electrochemical energy storage.[27–32] Porous polyimides not only inherit mechanical strength, thermal stability and chemical resistance from polyimides,[33] but also gain delicately designed porosity and functionality. Among various PIs, polyetherimide (PEI) attracts extensive interests because of the excellent combination of high thermomechanical performance and good processability, in both solution and melt processings.[33] Conventionally, porous PEI and PI in general are prepared by synthesis of covalent organic frameworks,[1,7–11,34] introduction of porogens,[23,27,31,35–48] utilization of phase inversion,[2,5,23,36,49,50] electrospinning,[28–30,51,52] and thermolysis of block or graft copolymers.[22,53–65] These methods often yield microporous (pore width <2 nm) or macroporous structures (pore width >50 nm). However, the preparation of PEI and PI in general with mesoporous structures (2–50 nm) *via* environmentally benign methods remains a challenge.

Among the various methods for preparing porous structures, covalent organic frameworks stand out for preparing micropores. For instance, trigonal/tetrahedral centers and rigid linkers can crosslink and construct polyimide frameworks with intrinsic micropores.[7–11,34] The topology of frameworks and length of linkers, however, limit the pore size to be smaller than 3 nm.[7–9,34] Alternatively, porogens with predefined sizes are well-suited for templating pores. The porogens are initially embedded in a polymer matrix and then eliminated to create pores. Various porogens and eliminating methods have been developed, including SiO_2 nanospheres *via* HF etching,[27,31,35–37] salts or dibutyl phthalate *via* solvent extraction,[38–41] solvents *via* freeze-drying (or lyophilization),[44,45] polymer blends *via* thermolysis,[42,43] and isocyanates generating CO_2 to induce foaming.[23,46,47] In these systems, the porogens often aggregate into macro-scale domains, therefore resulting in macropores. Similarly, in wet phase inversion-induced pore generation, the non-solvents occupy volumes within wet polymer films as macro-scale domains and thus create macropores.[23,36,49,50] Lastly, electrospinning produces inter-fiber voids in fiber mats during processing, and hence the pore sizes are also in macro-scales.[28–30,51]

[a]*Department of Chemistry, Virginia Tech, Blacksburg, Virginia 24061, USA. E-mail: gliu1@vt.edu*
[b]*Department of Chemical Engineering, Virginia Tech, Blacksburg, Virginia 24061, USA*
[c]*Macromolecules Innovation Institute, Virginia Tech, Blacksburg, Virginia 24061, USA*
[d]*Division of Nanoscience, Academy of Integrated Science, Virginia Tech, Blacksburg, Virginia 24061, USA*

†Electronic supplementary information (ESI) available. See DOI: 10.1039/d1py00601k

Different from the above methods that cannot reliably produce mesopores, block or graft copolymers are capable of microphase-separation to form mesoscale domains, holding great promise for preparing mesoporous structures.[62,63] Various thermally labile polymers have been employed to synthesize block or graft copolymers of PEI and PI in general, including polystyrene,[54,66] poly(α-methyl styrene),[55,56] poly(ethylene oxide),[57] poly(propylene oxide),[53,58–61] poly(methyl methacrylate),[62,63] polycaprolactone,[22,64,65,67] *etc*. After microphase separation, the thermally labile polymers are thermalized to create pores. However, gaseous species, which are produced by decomposition of the labile phase, often detrimentally plasticize the polymer matrix, even for PI with high glass transition temperatures (T_g). The gaseous species blow across the softened polymer matrix to create porous structures.[54,68] The pore sizes, albeit smaller than those created by porogens, phase inversion, and electrospinning, remain in the range of hundreds of nanometers.[22,53–65] Therefore in the fabrication of mesoporous polymers, it is critical to avoid the blowing effect from thermolysis while removing the labile phase.

Herein, we report the use of hydrolysis to prepare mesoporous PEI from triblock copolymers of polylactide-*b*-polyetherimide-*b*-polylactide (AIA). Polylactide (PLA) was chosen as the labile phase because of its susceptibility to hydrolysis. Under mild conditions of pH ~7.4 at 70 °C, PLA decomposed to water-soluble species, *i.e.*, potassium lactate, without producing any gaseous species to plasticize PEI, resulting in mesoporous PEI films with an average pore size of 24 nm. We found that the mesoporous PEI films prepared by hydrolysis exhibited storage moduli (E') of about 1 GPa at room temperature, and glass transition temperatures (T_g) higher than 230 °C in thermodynamic tests.

Experimental

Materials

4,4′-(4,4′-Isopropylidenediphenoxy)bis(phthalic anhydride) (*a.k.a.* 4,4′-bisphenol A dianhydride, BPADA) and *m*-phenylenediamine (mPD) were purchased from Sigma-Aldrich and purified as follows. In a nitrogen stream, the BPADA was melted at 200 °C and then cooled down to room temperature to eliminate moisture. The mPD was sublimated into white crystals at 70 °C under reduced pressure. Stannous 2-ethylhexanoate ($Sn(Oct)_2$), D,L-lactide, *o*-dichlorobenzene (oDCB), and phosphate buffer solution (1.0 M, pH ~7.4 at 25 °C) were purchased from Sigma-Aldrich and used as received. Deuterated chloroform ($CDCl_3$) was purchased from Cambridge Isotope Laboratories, Inc., and used as received. Dimethylformamide (DMF, HPLC grade) and lithium bromide (LiBr) were purchased from Fisher Scientific.

Instrumentation

Proton nuclear magnetic resonance (^{1}H NMR) spectra were collected on a Varian Unity at 400 MHz in $CDCl_3$. Size exclusion chromatography (SEC) was performed on a Tosoh EcoSEC HLC-8320 equipped with a refractive index detector, using DMF containing 0.05 M of LiBr as the eluent at a flow rate of 0.5 mL min^{-1}. Thermogravimetric analysis (TGA) was performed on a TA 5500 (TA Instruments) under air atmosphere. Scanning electron microscopy (SEM) was performed on a LEO Zeiss 1550 at an acceleration voltage of 2 kV and a working distance of ~4 mm. Oxygen plasma was conducted on a South Bay Technology PC-2000 with ultra-pure oxygen. Nitrogen adsorption isotherm was performed on a Micromeritics 3Flex Adsorption Analyzer. All the porous films were degassed at 120 °C for 1000 min to remove moisture. The specific surface area was calculated based on Brunauer–Emmett–Teller (BET) theory, and the pore size distribution was determined using nonlocal density functional theory (NLDFT). Dynamic mechanical analysis (DMA) was performed on a TA Q800 with a ramp rate of 3 °C min^{-1}, a strain of 0.1% and a frequency of 1 Hz.

Synthesis of PEI-NH_2

Amine-terminated PEI (PEI-NH_2) was synthesized *via* condensation polymerization (Scheme 1). In a typical synthesis of PEI-NH_2 with a number average molecular weight (M_n) of 45 kDa (denoted as PEI-45), BPADA (10 000.0 mg) and mPD (2105.3 mg) were added to a three-necked round bottom flask (500 mL) equipped with a mechanical stirrer, a Dean–Stark trap, and a nitrogen inlet with a constant flow of nitrogen. Subsequently, oDCB (100 mL) was added, then the resulting slurry mixture was immersed in an oil bath at 180 °C and reacted for 12 h with nitrogen purging. Afterward, the amber-colored solution was heated to 230 °C with constant nitrogen purging for one hour to remove the solvent. The viscous product was cooled down to room temperature and then dissolved in chloroform (100 mL). The resulting solution was added dropwise into methanol (1 L). A yellowish precipitate

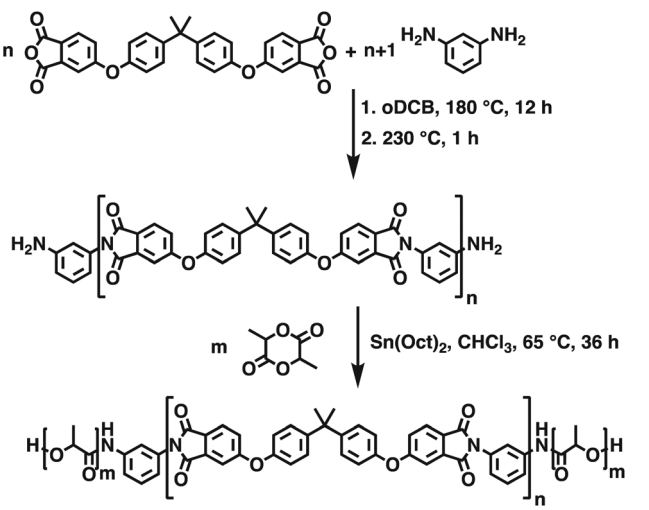

Scheme 1 Synthesis of AIA. PEI-NH_2 was synthesized *via* condensation polymerization of BPADA and mPD. The amine end groups in PEI initiated ring-opening polymerization of PLA to produce AIA triblock copolymers.

was collected *via* vacuum filtration and dried at 220 °C overnight *in vacuo*.

Synthesis of PLA-*b*-PEI-*b*-PLA (AIA)

AIA was synthesized *via* ring-opening polymerization of lactide using PEI-NH_2 as a macro-initiator (Scheme 1).[69] To synthesize AIA with a PLA weight fraction of 40% from PEI-45 (denoted as AIA-45), PEI-NH_2 (PEI-45, 500 mg) and lactide (1000 mg) were dissolved in anhydrous chloroform (20 mL) and added to a 100 mL Schlenk tube equipped with a magnetic stir bar. After degassing the solution *via* three freeze–pump–thaw cycles, Sn $(Oct)_2$ (10 mg) was added to the Schlenk tube in an argon-filled glovebox. The solution was set at 65 °C and reacted for 36 h. The viscous solution was cooled down to room temperature and precipitated in methanol. The resulting fine white powders were obtained *via* centrifugation and dried at 150 °C overnight *in vacuo*.

Preparation of AIA thin films

AIA (500 mg) was dissolved in chloroform (10 mL). The resulting solution was poured onto a glass slide (7 cm by 7 cm), and slowly dried in a desiccator for 2 days. The resulting thin film was baked at 150 °C overnight *in vacuo*.

Hydrolysis of AIA thin films

Both sides of AIA thin films were etched by oxygen plasma (2 min on each side) to remove the skin layers. The resulting films were then hydrolyzed in a phosphate solution (60 mL, 1.0 M) at 70 °C, following a previous report.[70] After hydrolysing for 1, 3, 5, 7 and 9 days, a small portion of AIA films (~20 mg) were sampled for compositional and morphological characterizations using ^{1}H NMR and SEM, respectively, to investigate the hydrolysis efficiency. After 9-day hydrolysis, the resulting mesoporous PEI films were soaked in DI water to remove the absorbed buffer solution, and then dry at 80 °C overnight *in vacuo*.

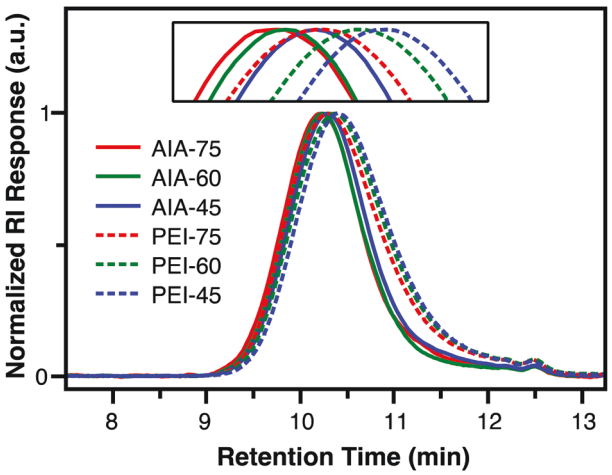

Fig. 1 SEC traces of AIA and the corresponding PEI macro-initiators. The shorter retention times of AIA than those of the corresponding PEI macro-initiator confirm the successful synthesis of AIA.

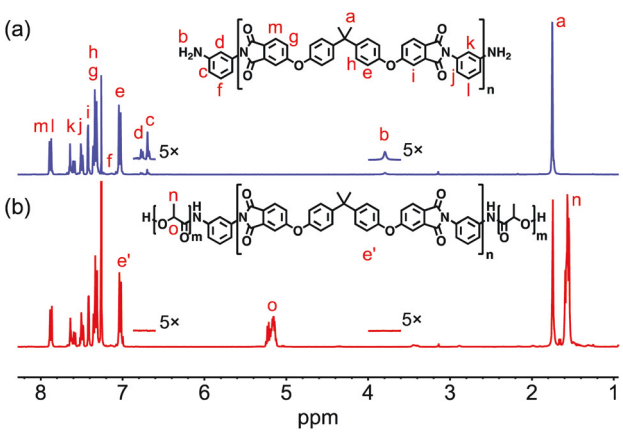

Fig. 2 Representative ^{1}H NMR spectra of (a) PEI-45 and (b) AIA-45. According to the integrated areas of peak o and e′, the weight fraction of PLA in AIA was 38.8%.

Results and discussion

Polymer molecular weight dictates the mechanical performance and thus the integrity of porous thin films. To investigate the effect of molecular weight on the mechanical strength of mesoporous PEIs, we synthesized three PEI-NH_2 macro-initiators (Scheme 1 and Table S1†) with molecular weights of 45, 60 and 75 kDa (designated PEI-45, -60 and -75, respectively; Fig. 1). The molecular structure was confirmed by ^{1}H NMR (Fig. 2a). From the three macro-initiators, we further synthesized three AIA block copolymers with a PLA weight fraction of ~40% (designated AIA-45, -60 and -75, respectively). SEC confirmed the conversion of PEI macro-initiators to AIA triblock copolymers (Fig. 1). The decreasing retention times from PEI-45 to PEI-75 indicated good control over the PEI molecular weights. After the polymerization of PLA, the retention time was shorter than that of the corresponding PEI, suggesting the successful incorporation of PLA onto the PEI chain ends. Noteworthy, the AIA SEC traces had smaller full widths at half maximum (FWHM) than the corresponding PEI macro-initiators. The smaller FWHM was a signature of the intrinsically better-controlled dispersity by ring-opening polymerization than condensation polymerization.

The weight fraction of PLA in AIA was calculated according to ^{1}H NMR spectrum (*i.e.*, AIA-45, Fig. 2b). Peak o at ~5.17 ppm was assigned to the methines in PLA repeating units, and peak e′ at ~7.14 ppm was assigned to the aromatic protons near the ether moieties in PEI repeating units. All other peaks were assigned, confirming the structure of block copolymer (Fig. 2a). The weight fraction of PLA in AIA was calculated according to eqn (1).

$$\varphi_{PLA} = \frac{I_o \times M_{PLA}}{I_o \times M_{PLA} + I_{e'}/4 \times M_{PEI}} \quad (1)$$

where φ_{PLA} is the weight fraction of PLA in AIA; I_o and $I_{e'}$ are the integral values of peak o and e′, respectively; M_{PLA} (72.1 Da) and M_{PEI} (592.6 Da) are the molecular weights of PLA and PEI repeating units. The integral ratio of peak o and peak e′ was measured to be 130 : 100, corresponding to a φ_{PLA} of 38.8%. Similarly, φ_{PLA} is 38.4% for AIA-60, and 38.2% for AIA-75.

The weight fraction of PLA in AIA was also confirmed by TGA (Fig. 3). The TGA traces of AIA exhibited two distinct weight loss regimes: the first regime (180–300 °C) was attributed to the thermal degradation of PLA,[71] while the second one (above 450 °C) was the decomposition of PEI.[72] The weight losses at 400 °C after PLA degradation were measured to be 39.8%, 38.1% and 38.0% for AIA-45, -60 and -75, respectively, in agreement with the φ_{PLA} determined from ^{1}H NMR. Noteworthy, the thermal decomposition of PLA overlapped the glass transition of PEI (typically ~217 °C (ref. 66)), which ruled out the use of thermolysis to create uniform porous structures. For example, AIA-45 had a 5% weight loss decomposition temperature ($T_{d,5\%}$) of 224 °C. If this temperature was used to thermalize PLA to create pores, the decomposition gaseous species would blow the softened PEI matrix to create nonuniform macropores, similar to the thermolysis process in previous reports.[54,68]

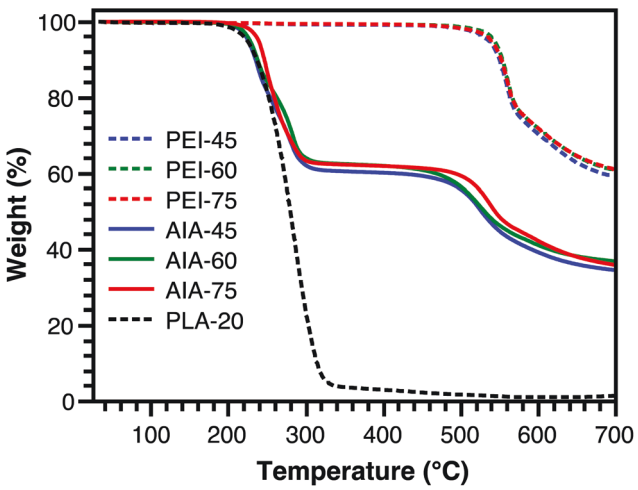

Fig. 3 TGA of AIA, PEI and PLA. The first and second weight loss of AIA at 180–300 °C and above 450 °C corresponded to the thermal decomposition of PLA and PEI, respectively. According to the weight loss, the weight fractions of PLA in AIA-45, -60 and -75 were 39.8%, 38.1% and 38.0%, respectively.

Instead of thermolysis, we have used hydrolysis to prepare mesoporous PEI thin films. AIA triblock copolymers formed thin films after solution casting on a glass slide. Subjected to oxygen plasma and subsequent hydrolysis in a phosphate solution, the microstructures of AIA films changed as the hydrolysis time was increased. The oxygen plasma treatment removed the skin layers of the films and facilitated the subsequent hydrolysis. After oxygen plasma etching, for instance, the AIA-45 thin film exhibited a rough surface due to the different etching rates of PLA and PEI. The PLA phase had a faster etching rate by oxygen plasma thus appeared dark (Fig. 4). After hydrolysis for 1 and 5 days, the PLA phase was further etched and developed into mesopores. After 9 days, the hydrolysis completed, generating well developed mesoporous structures (Fig. 4 and Fig. S6†). The pore sizes of mesoporous PEI (MP) films were further characterized using nitrogen sorption. Based on the isotherms, the BET surface areas of MP-45, -60 and -75 were 36, 42 and 61 $m^2\ g^{-1}$, respectively (Fig. 5a). All MP films exhibited an average pore width of 24 nm (Fig. 5b). This mesoscale pore size is prominently smaller than the pore sizes of conventional porous polyimides,[22,53–65] validating our hypothesis that the hydrolysis process avoids the blowing effect and creates uniform mesopores.

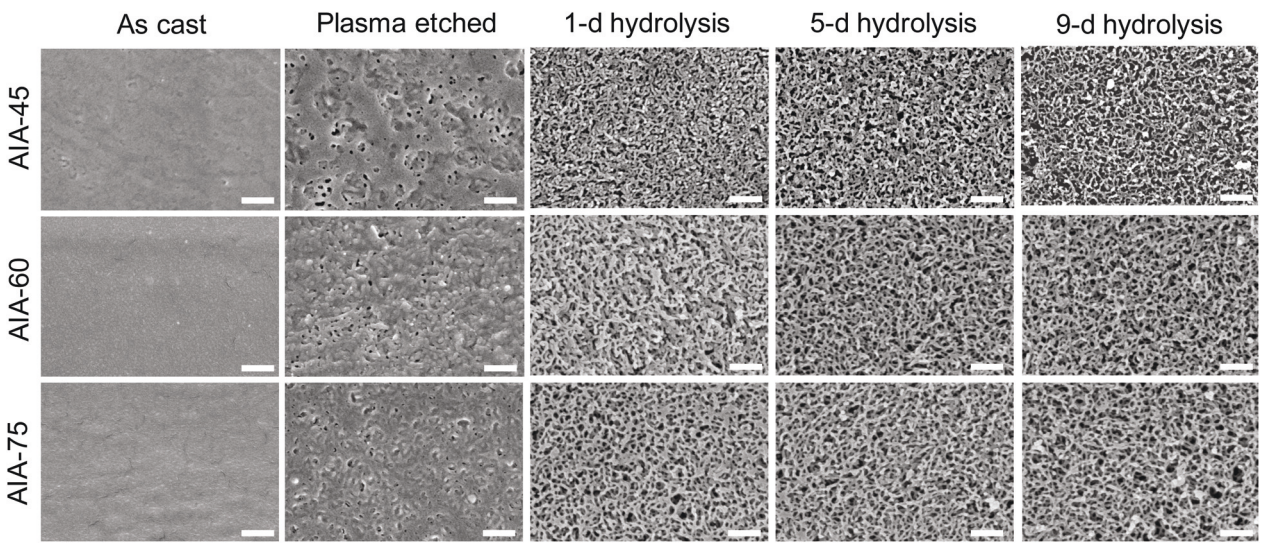

Fig. 4 Morphological evolution of AIA films. All scale bars, 300 nm.

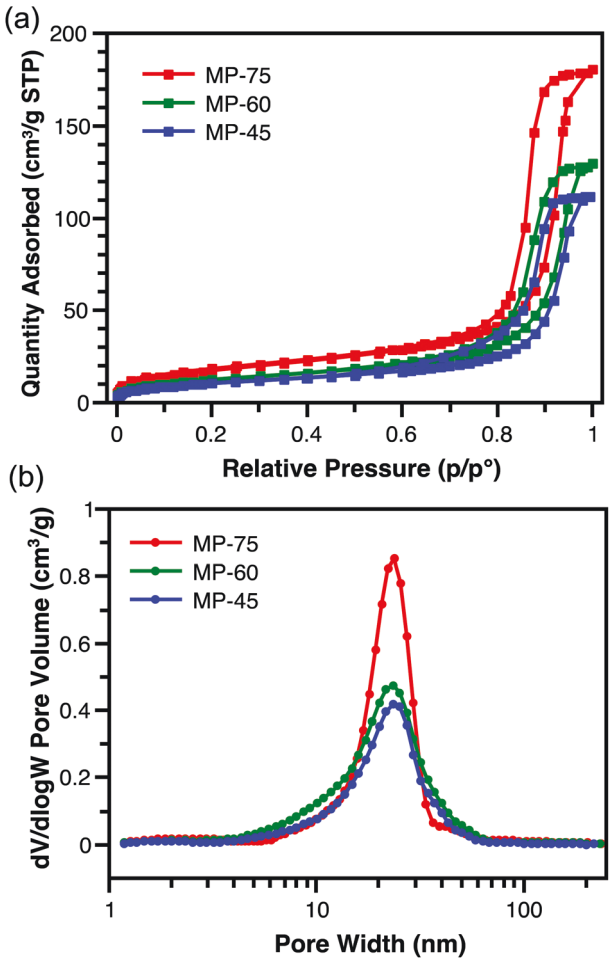

Fig. 5 Nitrogen sorption isotherms and pore size distributions of mesoporous PEI films. (a) The isotherms show specific surface areas of 36, 42 and 61 $m^2\ g^{-1}$ for MP-45, -60 and -75, respectively. (b) The pore size distributions display an average pore width of 24 nm for all MP films.

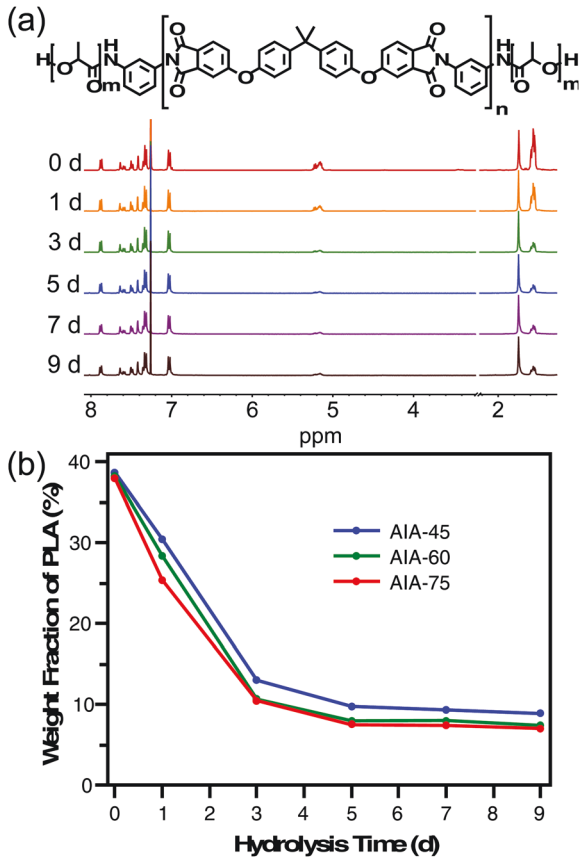

Fig. 6 Hydrolysis rate of AIA films in phosphate buffer solution. (a) ^{1}H NMR spectra display a decreasing signal of PLA repeating units in AIA-45. (b) The PLA weight fractions in all AIA films were below 9% after hydrolysis for 9 days.

The hydrolysis rate of PLA in AIA was investigated by measuring the amount of PLA residue using ^{1}H NMR after various lengths of hydrolysis time in phosphate buffer solutions (Fig. 6a). PLA showed a fast hydrolysis rate in the first 3 days. For instance, the PLA weight fraction in AIA-45 decreased from 38.8% to 13.0% (Fig. 6b). After hydrolysing for 9 days, the mesopores were well developed, and the weight fractions of residual PLA stabilized at 8.8%, 7.4% and 7.0% for AIA-45, -60 and -75, respectively.

After hydrolysis, the thermomechanical properties of mesoporous PEI (MP) films were evaluated using DMA. All MP films exhibited high storage moduli (E') and glass transition temperatures (T_g). At 30 °C, MP-45, -60 and -75 from AIA-45, -60, and -75 precursor films showed E' of 978, 1127 and 1216 MPa, respectively (Fig. 7a). The peaks of loss moduli (E'') at 217, 223 and 227 °C indicated the softening of PEI (Fig. 7b). Based on tan(δ), the glass transition temperatures were 233, 234 and 236 °C for MP-45, -60 and -75, respectively (Fig. 7c).

To prepare mesoporous PEI films *via* hydrolysis, three factors are essential. First, appropriate sacrificial domain sizes are an important starting point to create mesopores. In the case of using polymer blends or polymer/salt mixtures to prepare porous structures, the thermodynamically driven macrophase separation inevitably produces macro-scale domains that eventually lead to macropores after removing the sacrificial phase.[38–43] In contrast, block copolymer-based microphase separation ensures the formation of mesoscale domains, which ultimately create mesoporous structures.[66] Nevertheless, it is critical to remove the sacrificial phase without damaging the polymer matrix. Thus, the second important factor is well-controlled removal of the sacrificial phase. In previous reports,[22,53–66,68] thermolysis of polyimide-based block copolymers decomposes the sacrificial phase and produces gaseous species, which plasticize the softened polyimide matrix, and worse, blow the resulting structures into macropores. Conversely, in this work, hydrolysis of PLA *via* mild chain-scission removes the sacrificial phase without producing gas or softening the PEI matrix, avoiding the blowing effect that distorts and enlarges the mesopores. Third, the polymer matrix must be mechanically strong to support the mesoporous structure. After removing the sacrificial phase, the

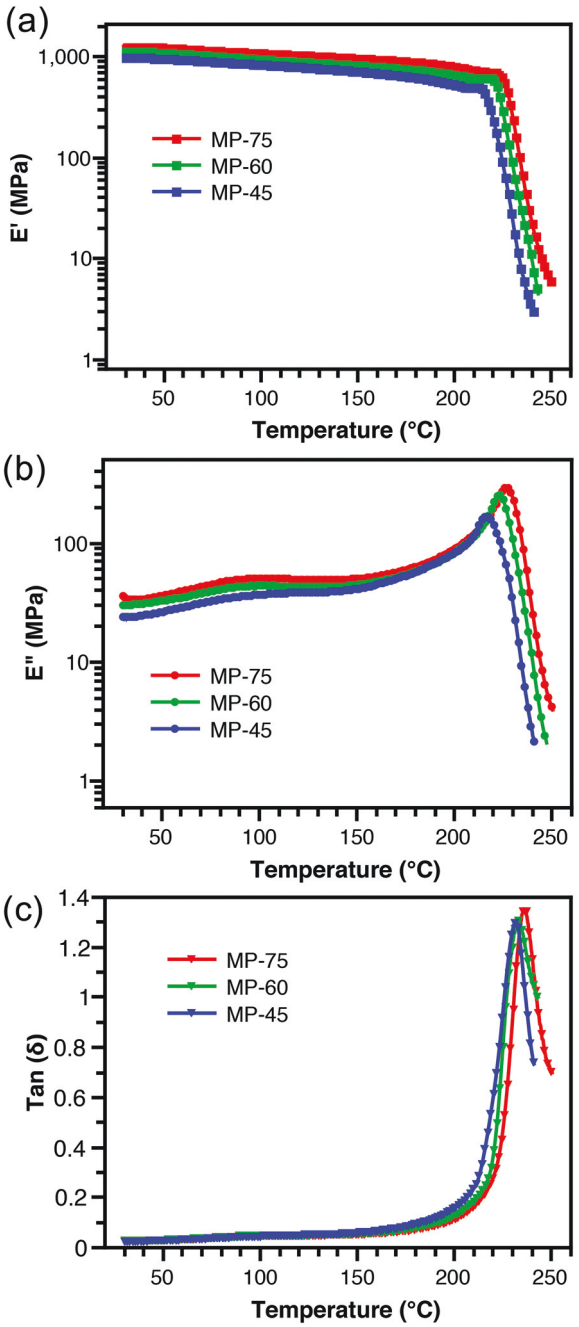

Fig. 7 Dynamic mechanical analysis of mesoporous PEI films after hydrolysis: (a) storage moduli, (b) loss moduli and (c) tan(δ) of MP-45, -60 and -75.

increasing pore volume reduces the overall mechanical strength of the films. A systematic investigation of the M_n of PEI and the resultant porous structures reveals that the PEI with M_n of 45 kDa and higher formed mesoporous PEI with good thermomechanical performance. Porous films made from AIA with a M_n of the PEI block lower than 30 kDa appeared fairly brittle and the porous structures collapsed after complete hydrolysis (Table S1 and Fig. S1–S5†).

Conclusions

In this work, we produced mesoporous polyetherimide thin films with pore sizes of 24 nm *via* hydrolysis of AIA triblock copolymers, which were synthesized by growing PLA peripheral blocks from PEI-NH_2 macro-initiators. The SEC retention time decreased after converting PEI-NH_2 macro-initiators to AIA. The weight fraction of PLA in AIA was confirmed to be ~40% by both ^{1}H NMR and TGA. AIA was solution-cast into films. After oxygen plasma and hydrolysis to remove the PLA phase, AIA thin films became porous. The mesoporous PEI films exhibit outstanding thermomechanical performance with E' of ~1 GPa at RT and T_g above 230 °C. This work presents an effective strategy to prepare mesoporous PEI thin films. The hydrolysis method is adaptable to other high-performance polymers. The mesoporous thin films are expected to find applications in various fields such as battery separators to suppress dendrites in lithium batteries.

Conflicts of interest

There are no conflicts to declare.

Acknowledgements

This material is based upon work supported by the National Science Foundation under Grant No. DMR-1752611 and CMMI-1914565, and the American Chemical Society Petroleum Research Foundation Doctoral New Investigator Award. The authors acknowledge the use of facilities in Nanoscale Characterization and Fabrication Laboratory (NCFL) at the Institute for Critical Technology and Applied Science (ICTAS), Virginia Tech.

Notes and references

1 G. Li and Z. Wang, *Macromolecules*, 2013, **46**, 3058–3066.
2 M. Niwa, H. Kawakami, T. Kanamori, T. Shinbo, A. Kaito and S. Nagaoka, *Macromolecules*, 2001, **34**, 9039–9044.
3 R. Swaidan, M. Al-Saeedi, B. Ghanem, E. Litwiller and I. Pinnau, *Macromolecules*, 2014, **47**, 5104–5114.
4 R. Swaidan, B. Ghanem, M. Al-Saeedi, E. Litwiller and I. Pinnau, *Macromolecules*, 2014, **47**, 7453–7462.
5 M. Iwase, A. Sannomiya, S. Nagaoka, Y. Suzuki, M. Iwaki and H. Kawakami, *Macromolecules*, 2004, **37**, 6892–6897.
6 Y. Zhuang, J. G. Seong, Y. S. Do, H. J. Jo, Z. Cui, J. Lee, Y. M. Lee and M. D. Guiver, *Macromolecules*, 2014, **47**, 3254–3262.
7 K. V. Rao, R. Haldar, T. K. Maji and S. J. George, *Polymer*, 2014, **55**, 1452–1458.
8 M. R. Liebl and J. Senker, *Chem. Mater.*, 2013, **25**, 970–980.
9 O. K. Farha, Y. S. Bae, B. G. Hauser, A. M. Spokoyny, R. Q. Snurr, C. A. Mirkin and J. T. Hupp, *Chem. Commun.*, 2010, **46**, 1056–1058.

10 H. Yao, N. Zhang, N. Song, K. Shen, P. Huo, S. Zhu, Y. Zhang and S. Guan, *Polym. Chem.*, 2017, **8**, 1298–1305.
11 J. Yan, B. Zhang and Z. Wang, *Polym. Chem.*, 2016, **7**, 7295–7303.
12 N. Song, T. Wang, H. Yao, T. Ma, K. Shi, Y. Tian, Y. Zou, S. Zhu, Y. Zhang and S. Guan, *Polym. Chem.*, 2019, **10**, 4611–4620.
13 A. S. Shaplov, S. M. Morozova, E. I. Lozinskaya, P. S. Vlasov, A. S. L. Gouveia, L. C. Tomé, I. M. Marrucho and Y. S. Vygodskii, *Polym. Chem.*, 2016, **7**, 580–591.
14 J. Zhang, X. Han, C. Yue, D. Liu, Z. Lin, Y. Sun, L. Chen, J. Pang and Z. Jiang, *Polym. Chem.*, 2020, **11**, 5057–5066.
15 Z. Pan, X. Zhang and X. Wang, *SN Appl. Sci.*, 2019, **1**, 239–248.
16 G. Zhao, X. Huang, Z. Tang, Q. Huang, F. Niu and X. Wang, *Polym. Chem.*, 2018, **9**, 3562–3582.
17 D. Zhang, T. Wang, Q. Wang and C. Wang, *J. Appl. Polym. Sci.*, 2017, **134**, 45106–45113.
18 L. Tian, C. Zhang, X. He, Y. Guo, M. Qiao, J. Gu and Q. Zhang, *J. Hazard. Mater.*, 2017, **340**, 67–76.
19 F. Topuz, M. A. Abdulhamid, S. P. Nunes and G. Szekely, *Environ. Sci.: Nano*, 2020, **7**, 1365–1372.
20 W. Zhu, X. Wang, T. Li, R. Shen, S.-J. Hao, Y. Li, Q. Wang, Z. Li and Z.-G. Gu, *Polym. Chem.*, 2018, **9**, 1430–1438.
21 Y. Jin, J. Tang, J. Hu, X. Han, Y. Shang and H. Liu, *Colloids Surf., A*, 2011, **392**, 178–186.
22 J. Ju, Q. Wang, T. Wang and C. Wang, *J. Colloid Interface Sci.*, 2013, **404**, 36–41.
23 M. A. Meador, C. R. Aleman, K. Hanson, N. Ramirez, S. L. Vivod, N. Wilmoth and L. McCorkle, *ACS Appl. Mater. Interfaces*, 2015, **7**, 1240–1249.
24 M. A. B. Meador, S. Wright, A. Sandberg, B. N. Nguyen, F. W. Van Keuls, C. H. Mueller, R. Rodríguez-Solís and F. A. Miranda, *ACS Appl. Mater. Interfaces*, 2012, **4**, 6346–6353.
25 K. R. Carter, H. J. Cha, R. A. Dipietro, C. J. Hawker, J. L. Hedrick, J. W. Labadie, J. E. McGrath, T. P. Russell, M. I. Sanchez, S. A. Swanson, W. Volksen and D. Y. Yoon, *MRS Proc.*, 2011, **381**, 79–91.
26 D. Chen, C. Liu, J. Tang, L. Luo and G. Yu, *Polym. Chem.*, 2019, **10**, 1168–1181.
27 Y. Shimizu and K. Kanamura, *J. Electrochem. Soc.*, 2019, **166**, A754–A761.
28 W. Jiang, Z. Liu, Q. Kong, J. Yao, C. Zhang, P. Han and G. Cui, *Solid State Ionics*, 2013, **232**, 44–48.
29 J. Lee, C.-L. Lee, K. Park and I.-D. Kim, *J. Power Sources*, 2014, **248**, 1211–1217.
30 Z. Zhou, T. Zhao, X. Lu, H. Cao, X. Zha and Z. Zhou, *J. Power Sources*, 2018, **396**, 542–550.
31 Y. Maeyoshi, D. Ding, M. Kubota, H. Ueda, K. Abe, K. Kanamura and H. Abe, *ACS Appl. Mater. Interfaces*, 2019, **11**, 25833–25843.
32 M. Nagasaki and K. Kanamura, *ACS Appl. Energy Mater.*, 2019, **2**, 3896–3903.
33 T. Takekoshi, in *New Polymer Materials*, Springer, Berlin Heidelberg, 1st edn, 1990, vol. 94, pp. 1–25.
34 Y. Luo, B. Li, L. Liang and B. Tan, *Chem. Commun.*, 2011, **47**, 7704–7706.
35 Q. Wang, C. Wang and T. Wang, *J. Colloid Interface Sci.*, 2013, **389**, 99–105.
36 H. Wang, T. Wang, S. Yang and L. Fan, *Polymer*, 2013, **54**, 6339–6348.
37 H. Munakata, D. Yamamoto and K. Kanamura, *J. Power Sources*, 2008, **178**, 596–602.
38 Z. Li, H. Zou and P. Liu, *RSC Adv.*, 2015, **5**, 37837–37842.
39 J.-M. Xiao, X.-C. Shang and L.-P. Qin, *Int. J. Miner., Metall. Mater.*, 2010, **17**, 782–785.
40 S. Chisca, I. Sava and M. Bruma, *Polym. Int.*, 2013, **62**, 1634–1643.
41 K. Taki, K. Hosokawa, S. Takagi, H. Mabuchi and M. Ohshima, *Macromolecules*, 2013, **46**, 2275–2281.
42 Z. Chen, D. Zhu, F. Tong, X. Lu and Q. Lu, *ACS Appl. Polym. Mater.*, 2019, **1**, 2189–2196.
43 H.-Z. Zhou, M.-S. Zhan, K. Wang and X.-Y. Liu, *High Perform. Polym.*, 2012, **25**, 33–41.
44 J. Choi, K. Yang, H. S. Bae, I. Phiri, H. J. Ahn, J. C. Won, Y. M. Lee, Y. H. Kim and M. H. Ryou, *Nanomaterials*, 2020, **10**, 1976.
45 M. Liu, Y. Wang, J. Ji, X. Chang, Q. Xu, X. Liu and J. Qin, *Mater. Lett.*, 2020, **267**, 127558.
46 S. Kanehashi, S. Sato and K. Nagai, in *Membrane Gas Separation*, ed. Y. Yampolskii and B. Freeman, John Wiley and Sons, 1st edn, 2010, ch. 1, pp. 1–27.
47 X.-Y. Liu, M.-S. Zhan and K. Wang, *J. Appl. Polym. Sci.*, 2013, **127**, 4129–4137.
48 M. Hernández-Guerrero and M. H. Stenzel, *Polym. Chem.*, 2012, **3**, 563–577.
49 Y. Ren and D. C. C. Lam, *J. Electron. Mater.*, 2008, **37**, 955–961.
50 Y. Taketani, S. Nagaoka and H. Kawakami, *J. Appl. Polym. Sci.*, 2004, **92**, 3016–3021.
51 L. Wang, N. Deng, L. Fan, L. Wang, G. Wang, W. Kang and B. Cheng, *Mater. Lett.*, 2018, **233**, 224–227.
52 S. Jiang, Y. Chen, G. Duan, C. Mei, A. Greiner and S. Agarwal, *Polym. Chem.*, 2018, **9**, 2685–2720.
53 J. L. Hedrick, K. Carter, M. Sanchez, R. D. Pietro and S. Swanson, *Macromol. Chem. Phys.*, 1997, **198**, 549–559.
54 J. L. Hedrick, C. J. Hawker, R. DiPietro, R. Jérôme and Y. Charlier, *Polymer*, 1995, **36**, 4855–4866.
55 J. L. Hedrick, R. DiPietro, C. J. G. Plummer, J. Hilborn and R. Jérôme, *Polymer*, 1996, **37**, 5229–5236.
56 Y. Charlier, J. L. Hedrick, T. P. Russell, S. Swanson, M. Sanchez and R. Jérôme, *Polymer*, 1995, **36**, 1315–1320.
57 L. Wang, J. Lu, M. Liu, L. Lin and J. Li, *Particuology*, 2014, **14**, 63–70.
58 J. L. Hedrick, T. P. Russell, J. Labadie, M. Lucas and S. Swanson, *Polymer*, 1995, **36**, 2685–2697.
59 C.-M. Chung, J.-H. Lee, S.-Y. Cho, J.-G. Kim and S.-Y. Moon, *J. Appl. Polym. Sci.*, 2006, **101**, 532–538.
60 Y. Charlier, J. Hedrick and W. Volksen, *Polymer*, 1995, **36**, 987–1002.
61 K. R. Carter, R. A. DiPietro, M. I. Sanchez and S. A. Swanson, *Chem. Mater.*, 2001, **13**, 213–221.

62 S. Miyata, K. Yoshida, H. Shirokura, M. Kashio and K. Nagai, *Polym. Int.*, 2009, **58**, 1148–1159.
63 G. D. Fu, B. Y. Zong, E. T. Kang, K. G. Neoh, C. C. Lin and D. J. Liaw, *Ind. Eng. Chem. Res.*, 2004, **43**, 6723–6730.
64 J. L. Hedrick, T. P. Russell, M. Sanchez, R. DiPietro and S. Swanson, *Macromolecules*, 1996, **29**, 3642–3646.
65 T. K. Meleshko, A. V. Kashina, N. N. Saprykina, S. V. Kostyuk, I. V. Vasilenko, P. A. Nikishev and A. V. Yakimanskii, *Russ. J. Appl. Chem.*, 2017, **90**, 602–612.
66 D. Guo, A. U. Khan, T. Liu, Z. Zhou and G. Liu, *Polym. Chem.*, 2019, **10**, 379–385.
67 C. Liu, B. Liu and M. B. Chan-Park, *Polym. Chem.*, 2017, **8**, 674–681.
68 S. Ando, A. Yoshida and K. Nagai, *Polym. Eng. Sci.*, 2016, **56**, 1191–1200.
69 M. Ju, F. Gong, S. Cheng and Y. Gao, *Int. J. Polym. Sci.*, 2011, **6**, 1–7.
70 S. Li and S. McCarthy, *Biomaterials*, 1999, **20**, 35–44.
71 T. Ohkita and S.-H. Lee, *J. Appl. Polym. Sci.*, 2006, **100**, 3009–3017.
72 F. Huang, X. Wang and S. Li, *Polym. Degrad. Stab.*, 1987, **18**, 247–259.